

Detection of systematic errors in quantum experiments

Tobias Moroder,^{1,2} Matthias Kleinmann,¹ Philipp Schindler,³ Thomas Monz,³ Otfried Gühne,^{1,2} and Rainer Blatt^{2,3}

¹Naturwissenschaftlich-Technische Fakultät, Universität Siegen, Walter-Flex-Str. 3, D-57068 Siegen, Germany

²Institut für Quantenoptik und Quanteninformatik,

Österreichische Akademie der Wissenschaften, Technikerstr. 21A, A-6020 Innsbruck, Austria

³Institut für Experimentalphysik, Universität Innsbruck, Technikerstr. 25, A-6020 Innsbruck, Austria

When systematic errors are ignored in an experiment, the subsequent analysis of its results becomes questionable. We develop tests to identify systematic errors in experiments where only a finite amount of data is recorded and apply these tests to tomographic data taken in an ion-trap experiment. We put particular emphasis on quantum state tomography experiments and present two detection methods; the first relies on ideas similar to entanglement witnesses or Bell inequalities while the second is based on the generalized likelihood ratio test.

PACS numbers: 03.65.-w, 03.65.Wj, 42.50.Dv

Introduction.—Measurements are central to acquiring information about the underlying system in any quantum experiment. However, in particular for quantum systems of increased complexity, the analysis of all measurement data gets challenging when one deals with both statistical and systematic errors. Statistical errors refer to the intrinsic problem that true probabilities, as predicted by the laws of quantum mechanics, are never accessible in any real experiment but are merely approximated from count rates which lead to relative frequencies. A well-known example where such statistical effects play a dominant role is in quantum state tomography [1]: the task to determine a previously unknown state by means of appropriate measurements. Here the deviations between probabilities and relative frequencies cause severe problems in the actual state reconstruction, since naively using the frequencies in Born’s rule easily leads to unphysical “density operators”, meaning that some eigenvalues are negative. This problem can be circumvented using reconstruction principles that explicitly account for these statistical effects [2, 3].

The analysis is generally more complicated because of additional systematic errors, *e.g.*, drifts in the state generation, misalignment in the measurements or fluctuations of external parameters in the setup. In order to reconstruct the state from the observed data one requires an operator assignment for each classical outcome of the performed measurements. This measurement model is essential, not just for quantum state tomography, but also to certify state characteristics like entanglement via entanglement witnesses [4] or in applications like quantum key distribution to prove security in the calibrated device scenario [5]. However, in a real experiment the measured observables (and its independent repetitions) might deviate from this employed description due to some systematic errors. This mismatch can have severe impact on the analysis outcome and can lead to, for example, spurious entanglement detection [6], apparent violation of a Bell inequality [7] or complete insecurity in quantum key distribution [8, 9]. Though deviations of this kind have been discussed and partially counter-measured by different techniques [10–14], it has not yet been investigated

how to distinguish them from statistical errors. An exception is given in Ref. [15], where drift in a source is detected using measurements on subsequent states.

In this paper we present experimentally and theoretically two methods to detect whether systematic errors are statistically significant, *i.e.*, if there is only a small probability that such observed data were generated by statistical effects. In this case further analysis becomes irrelevant and the data can be rejected directly. Consequently, we strongly encourage that these tests are applied before reconstructing actual quantum states. We want to emphasize that these techniques can only falsify the assumptions but never serve as a justification that systematic errors are absent. Two procedures are presented, the first resembles the concept of entanglement witnesses [16, 17] and hence directly makes use of the structure of quantum states, while the second is based on the generalized likelihood ratio test [18, 19]. Let us point out that other procedures, like the prediction-based-ratio analysis of Ref. [20] or the chi-square goodness-of-fit [21], are other alternatives here.

Tomography setting.—A common tomography protocol is the Pauli measurement scheme [3] which has been used for n qubit systems in ion traps [22] or photonic setups [23]. Here for each of 3^n possible combinations of Pauli operators on n qubits one locally measures in the associated eigenbasis which provides 2^n distinct outcomes, thus in total $3^n \times 2^n = 6^n$ different outcomes. Note that an n qubit density operator is already determined by $4^n - 1$ real parameters, meaning that this measurement scheme collects largely over-complete data.

More generally, we consider a tomography protocol that performs measurements for different settings labelled by s and registers the respective frequencies $f_k^s = m_k^s/N_s$, where m_k^s denotes the counts of the specific outcome k in N_s repetitions of this experiment. The repetitions N_s are assumed to be equal for each setting. The attributed measurement operators to these classical data are denoted by M_k^s and have the property that they span the complete operator space in order to enable a full reconstruction of the unknown density operator. Most often, as is the case with the Pauli measurement scheme,

this set is over-complete, *i.e.*, the operators contain linear dependencies which can be expressed as linear identities $\sum c_k^s M_k^s = 0$ using real coefficients c_k^s . The set of probabilities consistent with this quantum tomography model are all distributions $P_{\text{qm}}(k|s) = \text{tr}(\rho M_k^s)$ that can be written using a density operator ρ .

Witness test.—The set of distributions consistent with the assumed quantum model can be characterized by linear inequalities. This is in analogy to entanglement witnesses [16, 17] for separable states or Bell inequalities [24] for local hidden variable models. Consider a set of real coefficients $w = w_k^s$ that define a positive semidefinite operator via $\sum w_k^s M_k^s = Z_w \succeq 0$, *i.e.*, all eigenvalues are non-negative. Then the expectation value of any probability distribution from the quantum model P_{qm} satisfies

$$w \cdot P_{\text{qm}} \equiv \sum_{s,k} w_k^s P_{\text{qm}}(k|s) = \text{tr}(\rho Z_w) \geq 0. \quad (1)$$

Thus a distribution P with $w \cdot P < 0$ is incompatible with the assumed quantum model, and any such distribution can indeed be detected by a witness of the described form (even with partial information [25]).

Equation (1) is formulated on the level of probabilities which are not accessible in the experiment. Nevertheless one can replace the probabilities by the observed frequencies $f = f_k^s$ and consider the sample mean value $w \cdot f \equiv \sum w_k^s f_k^s$ of the witness. Then $w \cdot f \geq 0$ does not need to hold anymore because statistical effects can produce a negative value. However, the probability to observe large deviations from the true mean is bounded and decreases exponentially with the number of performed repetitions. A quantitative statement is given by Hoeffding's tail inequality [26], as similarly used for example in efficient fidelity estimation [27, 28]. Let us emphasize that this inequality is even valid for small data sets containing only few or no counts for certain outcomes.

Proposition 1.—Consider a witness $w = w_k^s$ obeying $\sum w_k^s M_k^s = Z_w \succeq 0$. If the data are generated by the quantum model $P_{\text{qm}}(k|s) = \text{tr}(\rho M_k^s)$, then for all $t > 0$,

$$\text{Prob}[w \cdot f \leq -t] \leq \exp(-2t^2 N_s / C_w^2) \quad (2)$$

with $C_w^2 = \sum_s (w_{\text{max}}^s - w_{\text{min}}^s)^2$, where $w_{\text{max/min}}^s$ are the optima for setting s over all outcomes k . A proof is given in the appendix.

The interpretation of this is as follows: Suppose that one carries out an experiment for an arbitrary but previously chosen witness w and fixed error probability α , that one still tolerates before one announces a systematic error, maybe $\alpha = 1\%$. Using Proposition 1 one can assign a minimal necessary violation given by $t_\alpha = \sqrt{-C_w^2 \log(\alpha) / 2N_s}$. If one now registers frequencies f_{obs} that beat this value $w \cdot f_{\text{obs}} \leq -t_\alpha$, then the probability that these data have originated from a quantum model by chance is less than α and one says that a systematic error is significant (at significance level α). Since error values α are often a matter of choice one states results in terms of the smallest error probability that would

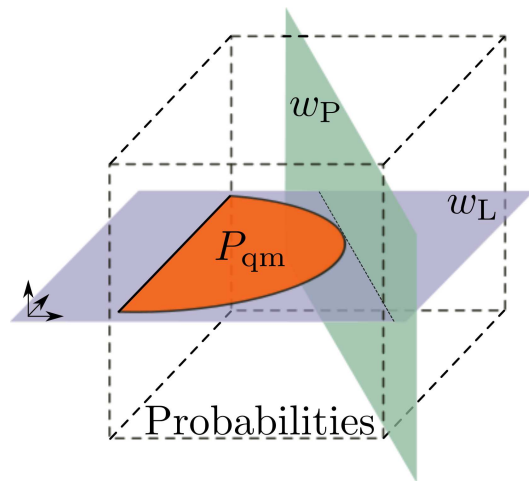


FIG. 1. (Color online) The admissible probabilities for the assumed quantum model P_{qm} form a convex, lower dimensional subset within all possible probability distributions (dashed cube). This depicted dimension reduction stems from the additional linear relations that a probability distribution from the quantum model must fulfil. The linear relations are checked by witnesses w_L . In contrast the witnesses w_P verify the positivity of the underlying density operator.

still allowed detection, hence $\exp[-2(w \cdot f_{\text{obs}})^2 N_s / C_w^2]$ if $w \cdot f_{\text{obs}} < 0$.

Witness structure.—Each above defined witness w can be decomposed into two conceptually different parts. One that solely verifies positivity of an underlying density operator, denoted as w_P in the following, and into another part w_L that only checks the linear dependencies, such that one obtains in total $w = w_P + w_L$. It turns out that these two parts of the witness are orthogonal. Let us point out that the witness w_P uniquely describes the operator $\sum w_{Pk}^s M_k^s = Z_w$, while the witness w_L (and also $-w_L$) vanishes $\sum w_{Lk}^s M_k^s = 0$ because of the linear dependencies. Figure 1 gives a schematic picture of this situation.

Issue of negative eigenvalues.—The above framework provides an answer to the issue of negative eigenvalues in linear inversion, since it is connected to witnesses of the type w_P . Linear inversion refers to the state reconstruction process in which one estimates the unknown density operator of the system by using the observed frequencies in Born's rule $\text{tr}(M_k^s \rho) = f_k^s$. Since this set of linear equations is typically not exactly solvable because of over-completeness one selects the operator ρ_{ls} which minimizes the least squares, $\sum [f_k^s - \text{tr}(\rho_{\text{ls}} M_k^s)]^2$. Since one ignores the positivity constraint this operator ρ_{ls} will often represent an invalid density operator because some eigenvalues are negative, *i.e.*, $\langle \psi | \rho_{\text{ls}} | \psi \rangle < 0$. The following statement provides a bound on the probability of negative expectation values.

Proposition 2.—Let ρ_{ls} be the linear inversion using least squares and consider a given vector $|\psi\rangle$. If the data are generated by the quantum model $P_{\text{qm}}(k|s) =$

$\text{tr}(\rho M_k^s)$, then for all $t > 0$,

$$\text{Prob}[\langle \psi | \rho_s | \psi \rangle \leq -t] \leq \exp(-2t^2 N_s / C_w^2) \quad (3)$$

with C_w^2 as given in Proposition 1 computed from the unique w_P satisfying $\sum w_{P_k}^s M_k^s = |\psi\rangle\langle\psi|$. A proof is given in the appendix.

The interpretation of this result is as follows: The probability to successfully guess in advance a state $|\psi\rangle$ where ρ_s has a negative expectation value is exponentially suppressed.

Likelihood ratio test.—In addition to the attributed quantum model $P_{\text{qm}}(k|s) = \text{tr}(\rho M_k^s)$ we can also describe the observations with a more general model assumption of independent distributions $P_{\text{ind}}(k|s) = p_k^s \geq 0$ and $\sum_k p_k^s = 1$ for each setting s . The question whether the observed data are compatible with the assumed quantum model can now be addressed by comparing the maximal likelihoods of either model [18].

For that, we start from the likelihood for a distribution P given the observed data f , which then is

$$L(P) = \prod_{k,s} P(k|s)^{N_s f_k^s}, \quad (4)$$

ignoring the multinomial prefactor. A quantum state ρ_{ml} that maximizes the likelihood $L(P)$ is considered to be a good estimate for the physical state [1, 2]. In contrast, for the model with all independent distributions, the optimum is given by $p_k^s = f_k^s$. Since the quantum model is contained in this more general model, the likelihood of any quantum model can at best be equal to this optimal likelihood. Thus one finds $L(f) \geq L[\text{tr}(\rho_{\text{ml}} M_k^s)]$ or equivalently, a non-negative log-likelihood ratio $\lambda_{\text{qm}} = 2 \log L(f) - 2 \log L[\text{tr}(\rho_{\text{ml}} M_k^s)]$.

The likelihood ratio test is based on the observation, that if the data are indeed generated from the quantum model then the probability for outcomes which satisfy $\lambda_{\text{qm}} \geq t$ decreases rapidly if the value t exceeds a certain value. While in general the distribution of λ_{qm} is cumbersome to access, we here can transform our situation to a canonical structure, for which it is known that such a ratio is distributed according to a chi-square distribution [29]. This statement known as Wilks' theorem [30] can be applied directly if one performs the optimization (rather than over quantum models) over probabilities $P_{\text{nqm}}(k|s) = \text{tr}(X M_k^s)$ that can be written in terms of a Hermitian operator X . Note that X can have negative eigenvalues, indicated by the subscript “n”, while still obeying the positivity constraints $\text{tr}(X M_k^s) \geq 0$ for the measurements M_k^s . With X_{ml} being a corresponding optimum we now study the log-likelihood ratio

$$\lambda_{\text{nqm}} = 2 \log L(f) - 2 \log L[\text{tr}(X_{\text{ml}} M_k^s)]. \quad (5)$$

Proposition 3.—If the data are generated by the d -dimensional quantum model $P_{\text{qm}}(k|s) = \text{tr}(\rho M_k^s)$ with K outcomes for each of the S settings, then for all $t > 0$, as $N_s \rightarrow \infty$,

$$\text{Prob}[\lambda_{\text{nqm}} \geq t] \rightarrow Q(\Delta/2, t/2), \quad (6)$$

with the dimension deficit $\Delta = (K - 1)S - (d^2 - 1)$ and the regularized incomplete gamma function Q [31]. A proof is given in the appendix.

The interpretation and application of this result is analogous to Proposition 1. Though Proposition 3 is only a strict statement in the asymptotic case $N_s \rightarrow \infty$, Eq. (6) gives reliable values already for moderately large N_s , as we will demonstrate below.

Experimental setup—Experimentally, we study tomographic data from an ion-trap quantum processor. Our system consists of a string of $^{40}\text{Ca}^+$ ions confined in a linear Paul trap where each ion represents a qubit. The quantum information is encoded in the $S_{1/2}(m=-1/2)$ ground state $|1\rangle$ and the metastable $D_{5/2}(m=-1/2)$ state $|0\rangle$. More details on the experimental parameters can be found in Ref. [32]. Qubit manipulation is performed by a series of laser pulses, adjusted by frequency, duration, intensity, and phase. Collective operations are of the form $\exp(-i\theta S_\phi/2)$ with $S_\phi = \sum_{l=1}^n \sigma_{\phi,l}$, $\sigma_{\phi,l} = \cos(\phi)\sigma_{x,l} + \sin(\phi)\sigma_{y,l}$ and $\sigma_{\cdot,l}$ the according Pauli operator acting on ion l . The rotation angle $\theta = \Omega\tau$ is defined by the global Rabi frequency Ω of all qubits and the duration τ of the laser pulse. Additionally, single ions can be addressed with a far off-resonantly detuned beam. Here the induced AC-Stark effect induces a rotation of the form $\exp(-i\theta\sigma_{z,l}/2)$ on ion l , with θ determined by the detuning, intensity and pulse duration. The combination of single-qubit phase rotations and collective S_ϕ rotations allows us to implement any local operation on the entire quantum register and, subsequently, to perform state tomography on a given state according to the Pauli measurement scheme.

The presented treatment of the implemented operations assumes homogeneous illumination via the global beam, *i.e.*, an identical Rabi frequency for all ions, as well as a narrow beam for individual phase rotations that solely illuminates the addressed ion. In an experimental realization, the finite width of the focused beam results in residual ion-light interaction on next-neighbor qubits. The Rabi frequency of ion k when addressing ion j can be described by the addressing matrix $\Omega_{j,k}$. Thus the operation on the qubit register can then be written as

$$\exp(-i \sum_k \Omega_{j,k} \tau \sigma_{z,k} / 2). \quad (7)$$

The addressing quality can be quantified with a cross-talk parameter $\epsilon = \max_{j \neq k} (\Omega_{j,k} / \Omega_{j,j})$, which can be increased by defocusing the addressed laser beam.

Using this setup we perform tomography on various kinds of states and investigate whether the obtained data suffer from any kind of systematic errors. This includes data for Greenberger-Horne-Zeilinger states on 4 ions, $|GHZ\rangle = (|0000\rangle + |1111\rangle) / \sqrt{2}$, where we intentionally increased the cross-talk ϵ in order to test the presented techniques, a large data set on a two-qubit Bell state $|\psi^-\rangle = (|01\rangle - |10\rangle) / \sqrt{2}$ and measurements on the ground state $|SSSS\rangle = |1111\rangle$. Moreover we re-analyse observations on a W-state on 5 qubits, $|W\rangle =$

state	n	N_s	ϵ	w_L	w_P	LR	LR*
GHZ	4	750	20%*	97%	$\approx 10^{-6}\%$	$\approx 10^{-10}\%$	$\approx 10^{-9}\%$
		750	12%*	–	$\approx 10^{-7}\%$	0.024%	0.14%
		600	<3%	79%	81%	0.91%	4.1%
Bell	2	61650	<3%	–	–	50%	49%
SSSS	4	2600	†	48%	84%	0.037%	0.008%
BE	4	5200	<3%	99%	14%	35%	36%
W	5	100	4%	49%	91%	(0.081%)	5.5%

TABLE I. Analysis of experimental data. We use the data from 3 experiments preparing a GHZ-state on $n = 4$ qubits with different cross-talk parameter ϵ , data from a Bell-state on two qubits, the ground (SSSS) and a bound entangled state (BE) on 4 qubits and a W-state on 5 qubits. The number of events per measurement setting is shown in the column N_s . The columns w_L and w_P show the lowest error probabilities of the test given by Proposition 1, checking linear dependencies or positivity respectively, which would have allowed a systematic error detection, “–” stands for no detection. The column LR lists similar values according to Proposition 3, while LR* is obtained using a parametric bootstrapping method [34] with a 1000 samples. The bracketed value suffers from an insufficient number of samples. For data marked with * we manually increased the cross-talk, while † could have been intensity fluctuations.

$(|00001\rangle + |00010\rangle + |00100\rangle + |01000\rangle + |10000\rangle)/\sqrt{5}$ and a bound-entangled Smolin state [33].

Empirical findings.— At first we implement the witness test, see Table I. Let us stress that Proposition 1 does not allow us to determine and to evaluate the witness w from the same data. If one would do so then one effectively evaluates $\min_w w \cdot f$ instead of $w \cdot f$ as required in Proposition 1. Because of that we divide the observed data into two equally sized parts, yielding frequencies f_1 and f_2 . Afterwards we use the first part f_1 to determine a reasonable witness w , which is finally evaluated on the second data, $w \cdot f_2$. Here we choose either of the two types of witnesses testing positivity w_P or linear dependencies w_L . As witness w_P we select the witness that corresponds to the projector onto the smallest eigenvalue on the linear inversion ρ_{ls} using the first data set f_1 . For the linear dependencies we use the witness $w_L = -f_1 + \text{tr}(\rho_{ls} M_k^s)$, because it gives the largest negative expectation value $w_L \cdot f_1$ on the first data. Let us point out, that the employed choices here might not be optimal [35]. If the observed value $w \cdot f_2$ is negative, we ask for the statistical significance as explained after Proposition 1, *i.e.*, we state the lowest error probability that would have still allowed detection via this witness test, $\exp[-2(w \cdot f_2)^2 N_s / C_w^2]$. Values as low as $10^{-5}\%$ are clearly unacceptable.

For our data, the witness w_P reliably detects the artificially introduced cross talk for the GHZ-state with parameters $\epsilon = 12\%$ and $\epsilon = 20\%$. In contrast, the witness w_L turns out to be less powerful for these examples.

The likelihood ratio test, which we investigate as second method, is best suited for a larger number of sam-

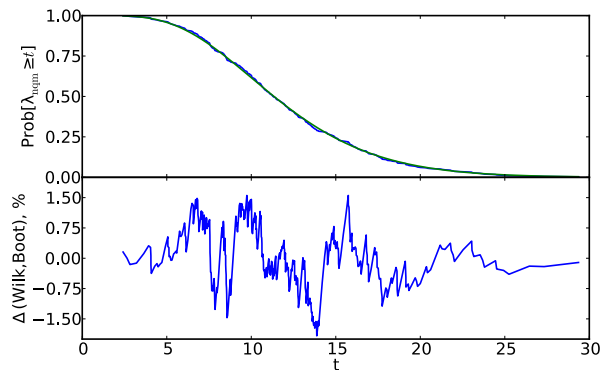


FIG. 2. (Color online) Distribution of the log-likelihood ratio (5) from a 411-fold repetition of a Bell-state tomography experiment. We show the fraction of runs having a log-likelihood ratio λ_{nqm} larger or equal to the specified value t . In the upper graph, the shaky blue line corresponds to the experimental data, while the smooth green line is the prediction according to Wilks’ theorem (6). The lower graph shows the difference between both curves. A simulation of the experiment yielded a similar result (not shown).

ples, since Proposition 3 makes strictly speaking only a statement for $N_s \rightarrow \infty$. In Figure 2 we compare the empirical distribution between a two-qubit Bell experiment using 150 samples/setting and the predicted distribution according to Wilks’ theorem. Hence for the two-qubit case this number might already be sufficiently close to this limit. This observation can be further supported via a comparison with a bootstrapping method [34] (see appendix) which mostly produces similar results as the ones obtained from Proposition 3. Based on these observations we are confident that the results using Proposition 3 for finite N_s are trustworthy for all data from Table I except for the W-state, which has a too low number of samples. Evaluating the experimental data we detect again the manually increased cross talk in the GHZ experiments, but now also some discrepancies in the SSSS experiment, which most likely occurred because of intensity fluctuations during the experiment [36].

Conclusion & Outlook.—The tomographic reconstruction of a quantum state can be problematic since non-physical properties, such as negative eigenvalues, might occur. One possible way out is to use reconstruction schemes, which by construction result in a valid state. Then, however, serious concerns remain, as the negative eigenvalues can be a signature of systematic errors. We have provided tests which can be used to distinguish systematic from statistical errors in quantum experiments. These tests were shown to recognize systematic errors in real tomographic data from ion trap experiments.

We formulated our result for the important case of state tomography, however, our methods can be applied to check other assumptions like the non-signaling condition in Bell experiments. From the more general perspective, many experiments in physics aim at determining the parameters in an assumed theoretical model. Our re-

sults show that it is possible to give rigorous estimates on whether the assumed model class is indeed appropriate or not.

Acknowledgments.— We thank K.M.R. Audenaert, K. Banaszek, M. Cramer, O. Gittsovich, S. Glancy, M. Guta, D. Gross, B. Jungnitsch, H. Kampermann, E. Knill, S. Niekamp and Y. Zhang for stimulating discussions. The authors are grateful for the opportunity to

participate in the Heraeus Summer School “Modern statistical methods in QIP”, where parts of this research have been developed. This work has been supported by the FWF (START prize Y376-N16, SFB-FOQUS), the EU (AQUITE, Marie Curie CIG 293993/ENFOQI), the BMBF (CHIST-ERA network QUASAR), the IARPA, the Institut für Quanteninformaton GmbH and by the European Research Council.

-
- [1] M. G. A. Paris and J. Řeháček, eds., *Quantum state estimation* (Springer Berlin Heidelberg, 2004).
- [2] Z. Hradil, Phys. Rev. A **55**, R1561 (1997).
- [3] D. F. V. James, P. G. Kwiat, W. J. Munro, and A. G. White, Phys. Rev. A **64**, 052312 (2001).
- [4] M. Lewenstein, B. Kraus, J. I. Cirac, and P. Horodecki, Phys. Rev. A **62**, 052310 (2000).
- [5] V. Scarani, H. Bechmann-Pasquinucci, N. J. Cerf, M. Dušek, N. Lütkenhaus, and M. Peev, Rev. Mod. Phys. **81**, 1301 (2009).
- [6] A. Acín, N. Gisin, and L. Masanes, Phys. Rev. Lett. **97**, 120405 (2006).
- [7] I. Gerhardt, Q. Liu, A. Lamas-Linares, J. Skaar, V. Scarani, V. Makarov, and C. Kurtsiefer, Phys. Rev. Lett. **107**, 170404 (2011).
- [8] B. Qi, C. H. F. Fung, H. K. Lo, and X. Ma, Quantum Inf. Comput. **7**, 73 (2007).
- [9] L. Lydersen, C. Wiechers, C. Wittmann, D. Elser, J. Skaar, and V. Makarov, Nature Photonics **4**, 686 (2010).
- [10] P. Lougovski, S. J. van Enk, K. S. Choi, S. B. B Papp, H. Deng, and H. J. Kimble, New J. Phys. **11**, 063029 (2009).
- [11] T. Moroder, O. Gühne, N. J. Beaudry, M. Piani, and N. Lütkenhaus, Phys. Rev. A **81**, 052342 (2010).
- [12] J. D. Bancal, N. Gisin, Y.-C. Liang, and S. Pironio, Phys. Rev. Lett. **106**, 250404 (2011).
- [13] T. Moroder and O. Gittsovich, Phys. Rev. A **85**, 032301 (2012).
- [14] D. Rosset, R. Ferretti-Schöbitz, J.-D. Bancal, N. Gisin, and Y.-C. Liang, “Imperfect measurements settings: implications on quantum state tomography and entanglement witnesses,” ArXiv:1203.0911.
- [15] L. Schwarz and S. J. van Enk, Phys. Rev. Lett. **106**, 180501 (2011).
- [16] M. Horodecki, P. Horodecki, and R. Horodecki, Phys. Lett. A **223**, 1 (1996).
- [17] B. Terhal, Phys. Lett. A **271**, 319 (2000).
- [18] K. Knight, *Mathematical statistics* (Chapman & Hall/CRC Press, 2000).
- [19] R. Blume-Kohout, J. O. S. Yin, and S. J. van Enk, Phys. Rev. Lett. **105**, 170501 (2010).
- [20] Y. Zhang, S. Glancy, and E. Knill, Phys. Rev. A **84**, 062118 (2011).
- [21] A. F. Mood, *Introduction to the theory of statistics* (McGraw-Hill Inc., 1974).
- [22] H. Häffner, W. Hänsel, C. F. Roos, J. Benhelm, D. Chekhal kar, M. Chwalla, T. Körber, U. D. Rapol, M. Riebe, P. O. Schmidt, C. Becher, O. Gühne, W. Dür, and R. Blatt, Nature **438**, 643 (2005).
- [23] N. Kiesel, C. Schmid, G. Tóth, E. Solano, and H. Weinfurter, Phys. Rev. Lett. **98**, 063604 (2007).
- [24] A. Peres, Found. of Phys. **29**, 589 (1999).
- [25] T. Moroder, M. Keyl, and N. Lütkenhaus, J. Phys. A: Math. Theor. **41**, 275302 (2008).
- [26] W. Hoeffding, J. Am. Stat. Assoc. **58**, 301 (1963).
- [27] S. T. Flammia and Y.-K. Liu, Phys. Rev. Lett. **106**, 230501 (2011).
- [28] M. P. da Silva, O. Landon-Cardinal, and D. Poulin, Phys. Rev. Lett. **107**, 210404 (2011).
- [29] A chi-square distribution with $\Delta \in \mathbb{N}$ degrees of freedom is the distribution given by the sum of squares of Δ independent, standard normal random variables Z_i (Gaussian with zero mean and unit variance), so the distribution of $\sum_{i=1}^{\Delta} Z_i^2$.
- [30] S. S. Wilks, *Mathematical statistics* (John Wiley & Sons, New York, London, 1962).
- [31] Explicitly, $Q(s, x) = \int_x^{\infty} y^{s-1} e^{-y} dy / \int_0^{\infty} y^{s-1} e^{-y} dy$; the function $1 - Q(\Delta/2, t/2)$ is the cumulative distribution function of a chi-square distribution with Δ degrees of freedom.
- [32] F. Schmidt-Kaler, H. Häffner, S. Gulde, M. Riebe, G. P. T. Lancaster, T. Deuschle, C. Becher, W. Hänsel, J. Eschner, C. F. Roos, and R. Blatt, Applied Physics B: Lasers and Optics **77**, 789 (2003).
- [33] J. T. Barreiro, P. Schindler, O. Gühne, T. Monz, M. Chwalla, C. F. Roos, M. Hennrich, and R. Blatt, Nature Physics **6**, 943 (2010).
- [34] B. Efron and R. J. Tibshirani, *An introduction to the bootstrap* (Chapman & Hall, 1994).
- [35] B. Jungnitsch, S. Niekamp, M. Kleinmann, O. Gühne, H. Lu, W. B. Gao, Y.-A. Chen, Z.-B. Chen, and J.-W. Pan, Phys. Rev. Lett. **104**, 210401 (2010).
- [36] The numerical optimizations that arise here are done using the solver `cp` from the package CVXOPT for the Python programming language.

APPENDIX

Proof of Proposition 1.—The proposition uses Hoeffding’s tail inequality [26] and the property that valid quantum distributions P_{qm} have a non-negative expectation value $w \cdot f \geq 0$ due to Eq. (1). Hoeffding’s inequality states that the sample mean $\bar{X} = \sum X_i/N$ of N independent, not necessarily identical distributed, bounded random variables X_i with $\text{Prob}[X_i \in [a_i, b_i]] = 1$ for $i = 1, \dots, N$ satisfies

$$\text{Prob}[\bar{X} - \mathbb{E}(\bar{X}) \leq -t] \leq \exp[-2N^2 t^2 / \sum (b_i - a_i)^2] \quad (8)$$

for all $t > 0$ and $\mathbb{E}(\bar{X})$ denoting the mean value of \bar{X} . In order to prove the proposition we identify \bar{X} with the sample mean of the witness. This is achieved as follows:

Suppose that Y_i^s denotes the random variable associated with the i -th repetition of the measurement setting s . In case of the measurement outcome k , Y_i^s takes the value Sw_k^s where S denotes the total number of measurement settings. It is bounded between $Y_i^s \in [Sw_{\min}^s, Sw_{\max}^s]$. Then the sample mean of all these variables

$$\bar{Y} = \frac{1}{SN_s} \sum_{s,i} Y_i^s \quad (9)$$

yields values

$$\frac{1}{SN_s} \sum_{s,k} Sw_k^s m_k^s = \sum_{s,k} w_k^s f_k^s = w \cdot f, \quad (10)$$

where m_k^s denotes the counts of the specific outcome k in N_s repetitions of the measurement settings s .

Using Hoeffding's inequality together with the property that $\mathbb{E}(\bar{Y}) = w \cdot P_{\text{qm}} \geq 0$ holds for any valid quantum distribution P_{qm} due to Eq. (1) one arrives at

$$\text{Prob}[w \cdot f \leq -t] = \text{Prob}[\bar{Y} \leq -t] \quad (11)$$

$$\leq \text{Prob}[\bar{Y} - \mathbb{E}(\bar{Y}) \leq -t] \quad (12)$$

$$\leq \exp[-2t^2 N_s / C_s^2], \quad (13)$$

with $C_s^2 = \sum_s (w_{\max}^s - w_{\min}^s)^2$. The first inequality holds because the set of all outcomes satisfying $\bar{Y} < -t$ is a subset of $\bar{Y} - \mathbb{E}(\bar{Y}) \leq -t$. This concludes the proof of the proposition.

Proof of Proposition 2.—In order to prove the proposition we show $\langle \psi | \rho_{1s} | \psi \rangle = w_{\text{P}} \cdot f$, which can then be used in Proposition 1 to obtain the final statement.

Given a valid decomposition w satisfying $\sum w_k^s M_k^s =$

$|\psi\rangle\langle\psi|$ one obtains

$$\langle \psi | \rho_{1s} | \psi \rangle = \sum w_k^s \text{tr}(M_k^s \rho_{1s}) = \sum w_k^s f_{\text{P}k}^s \quad (14)$$

$$= w \cdot f_{\text{P}} = w_{\text{P}} \cdot f, \quad (15)$$

together with the solution of least squares $\text{tr}(M_k^s \rho_{1s}) = f_{\text{P}k}^s$.

Proof of Proposition 3.—We start by a rough statement of Wilks' theorem (cf. *e.g.*, 13.8.1 in Ref. [30]). Suppose that we have a family of models, that is sufficiently smoothly parameterized by an open set $\Omega \subset \mathbb{R}^r$ and let A be a subspace of \mathbb{R}^r of dimension $r - \Delta$. If we draw N' samples from our model with some (unknown) parameter $z \in A \cap \Omega$, then the distribution of the log-likelihood ratio

$$\lambda_A = 2 \log \sup_{x \in \Omega} L(x) - 2 \log \sup_{y \in A \cap \Omega} L(y) \quad (16)$$

converges to the χ_{Δ}^2 distribution as $N' \rightarrow \infty$. Hence,

$$\lim_{N' \rightarrow \infty} \text{Prob}[\lambda_A \geq t] = Q(\Delta/2, t/2). \quad (17)$$

For our model, the set of parameters Ω is given by \tilde{p}_k^s with $k = 1, \dots, K-1$ obeying $\tilde{p}_k^s > 0$ and $\sum_k \tilde{p}_k^s < 1$. Furthermore, we let A be the subspace where $q_k^s = \text{tr}(X M_k^s)$ for some Hermitian matrix X . We now basically arrived at Proposition 3. It only remains to change the notation from \tilde{p}_k^s to p_k^s via $p_K^s = 1 - \sum_k \tilde{p}_k^s$ and to admit a more relaxed notation by essentially writing $\max_{x \in \bar{\Omega}}$ instead of $\sup_{x \in \Omega}$.

Bootstrapping for Table I.—We first calculate the maximum likelihood state ρ_{ml} from the measured data and then simulate the tomographic process using that state. From the simulated data we then calculate the log-likelihood ratio λ_{nqm} . We repeat this procedure 1000 times and compare the distribution with the predicted chi-square distribution. In our examples, the distribution matches always almost perfectly, however with a slightly different parameter Δ . We then determine Δ' to be such, that $Q(\Delta'/2, m) = 1/2$, where m is the median of the sampled distribution. Using Δ' , we obtain the values of the column LR* of Table I.